Numerical simulation of the gas heat conduction of aeroge materials

Yucong Li[1,*], *Shuai* Li[2] , *Lindong* Xia[1] , *Binbin* Liu[3] , *Weifeng* Jin[1], and *Yining* Zhu[1] ,

[1]PetroChina Jilin Petrochemical Company, Jilin, China
[2]Everbright Environmental Protection (China) Ltd, Shenzhen, China
[3]PowerChina Turbo Technology Company Ltd, Chengdu, China

Abstract. In order to obtain the gas heat conduction of aerogel materials, this paper applied lattice boltzmann method (LBM) to establish a microcosmic model D3Q15. Lattice Boltzmann method (LBM) was used to simulate the temperature distribution and had the advantage of simplifying calculation at the nano scale. Gas heat conduction would be effected by the size and boundary condition under nano-scale conditions. In this paper it can be concluded that the temperature jump under mirror rebound and diffuse reflection boundary was obvious as the value of t increasing from $8*10^{-12}$ to $4*10^{-9}$ and the mirror rebound boundary scattering increased drastically than diffuse reflection. the temperature jump would stay stable when the time arrived $4*10^{-9}$. As to diffuse reflection boundary, the effective thermal conductivity tended to decrease dramaticlly as r_b growing up.

1 Introduction

Nowadays, Thermal insulation materials shows the properties that high porosity, high surface area and low thermal conductivity and has palyed an important role in many fields, space vehicles, building envelope materials and so on[1]. The mechanisms of the heat transfer in aerogels are absolutely contributed on three modes which are solid heat conduction, gas heat conduction and thermal radiation[2], the gas heat conduction is higher mix of three modes in the heat transfer process. Therefore, in order to optimize aerogel structure and increase its thermal property, it is important to study the mechanism of gas heat conduction.

At present, the researchs on gas heat conduction properties of aerogel are mainly focused on three aspects, which are experimental measurement, theoretical analysis and numericael simulation[3]. The experimental measurement method can reflect the material properties directly but it is hard to measure the gas thermal conductivity at the micro/nano scale directly. the theoretical analysis methods mainly consist three models of Kaganer model[4], double-pore distribution model[5] and Zeng model[6] about gas heat conduction. the numerical simulations have been widely applied in recent years. The Lattice Boltzmann method(LBM) has the advantages of the temperature distribution of heat conduction at the

* Corresponding author: jh_liyucong@petrochina.com.cn

micro/nano scale, which cannot be obtained by traditional simulation methods Monte Carlo(MC) and Molecular Dynamics(MD)[7].

2 Physical and mathematical models

2.1 Three-dimensional physical model

Fig.1 displayed the gas heat conduction model of aerogels. The length, width and height of the model were expressed as L_x , L_y and L_z separately. The front and back walls are kept at a constant temperature T_1=300K and T_1=301K separately, others stayed adiabatic.

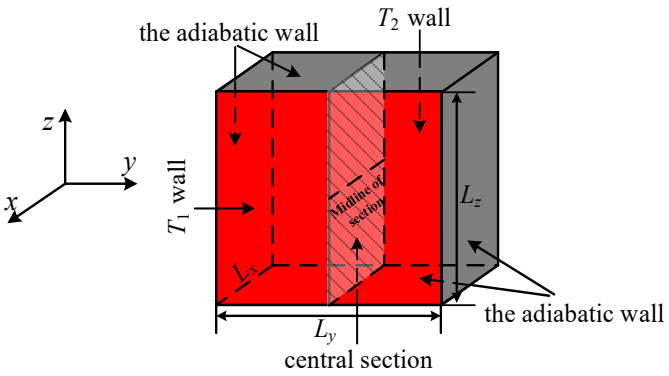

Fig. 1. Gas heat conduction model.

The equation was established to solve the gas heat conduction of aerogel for the three-dimensional ninteen-speed (D3Q15) model according to the following formula[8]:

$$f_i\left(r+e_i\delta t,t+\delta t\right)-f_i\left(r,t\right)=-\frac{1}{\tau}\left[f_i\left(r,t\right)-f_i^{eq}\left(r,t\right)\right] \tag{1}$$

where subscript i is discrete velocity directions of lattice point; r is the position vector; t is the time; δt is the time step size; e_i is the separate lattice velocity; τ is the dimensionless relaxation time; f_i is the internal energy distribution function; f_i^{eq} is the corresponding equilibrium distribution function.

$$f_i^{eq}=\begin{cases}\left(2/9\right)\rho c_pT, i=0\\ \left(1/9\right)\rho c_pT, i=1\sim 6\\ \left(1/72\right)\rho c_pT, i=7\sim 14\end{cases} \tag{2}$$

where T is temperature; ρ is the density of gas; c_p is the heat capacity ratio of air.

When the temperature becomes constant state, the effective thermal conductivity could be calculated by the following equation[9]:

$$\lambda_{eff}=\frac{L_x\int q\mathrm{d}A}{\Delta T\int \mathrm{d}A} \tag{3}$$

where L_x is the characteristic scale of heat flow direction, $\mathrm{d}A$ is the cross-sectional area for the heat flow, q is heat flux.

2.2 Boundary conditions

As a mesoscopic method, LBM expressed the distribution function as the collision migration process. The distribution function of the internal grid points could be obtained by the migration of adjacent grid points such as mirror rebound boundary, but some distribution functions at the boundary can not be determined by migration such as diffuse rebound boundary.

(1) Mirror rebound boundary

the mirror rebound boundary could be applied if there is no momentum exchange. This boundary can slide freely, The distribution function of the migration from the fluid grid point e_i to the boundary grid point is the symmetrical direction of the wall normal. so mirror rebound boundary was applied to no friction losses and the energy transfer free in these boundary condition, and the results would not be affected by the width L_y and the height L_z.

(2) Diffuse reflection boundary

In order to more realistically reflect the energy transfer between points and the boundaries, it is necessary to adopt diffuse reflection boundary. It assumes when the particles collide with the boundary, they would arbitrarily spread out in all directions. Therefore, the rebound scale factor r_b need to be considered when implementing this boundary format, it represent the proportion of particles that rebound along the original path when they interact with the boundary. Where r_b=1 was expressed as pure bounce treatment; meanwhile r_b=0.5 was ideal diffuse scattering; r_b=0 was pure mirror bounce. The specific forms were implemented as follow:

$$f_{i'}\left(r_b,t\right)=f_i\left(r_f,t\right) \tag{4}$$

where r_b was the boundary lattice point, $r_f=r_b-e_i\delta t$ was internal lattice point; $f_{i'}$ was a mirror-symmetric distribution function of f_i. The f_i could be obtained by the inner lattice points that was adjacent the boundary wall.

2.3 Program verification

The gas thermal conductivity of aerogel was numerically simulated within 10~80nm pore sizes, and compared with the results of the Zeng model and inference[10] in the same conditions. The Fig.2 showed that the results of this paper were the similar to the Zeng model but were slightly smaller than it. The result of the inference[10] showed deviate from this paper in 60~70nm because it only considered of particles impacting between atoms. To sum up, both of the simulation results have the same change trend, so the reliability of the LBM program could be proved.

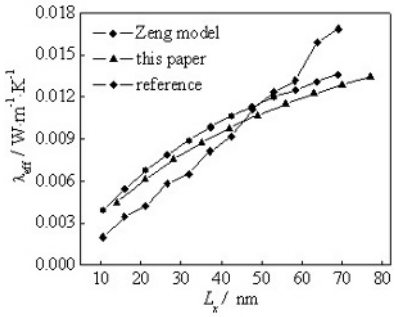

Fig. 2. Verification of numerical simulation results.

3 Results and discussion

3.1 Gas mirror rebound boundary temperature jump

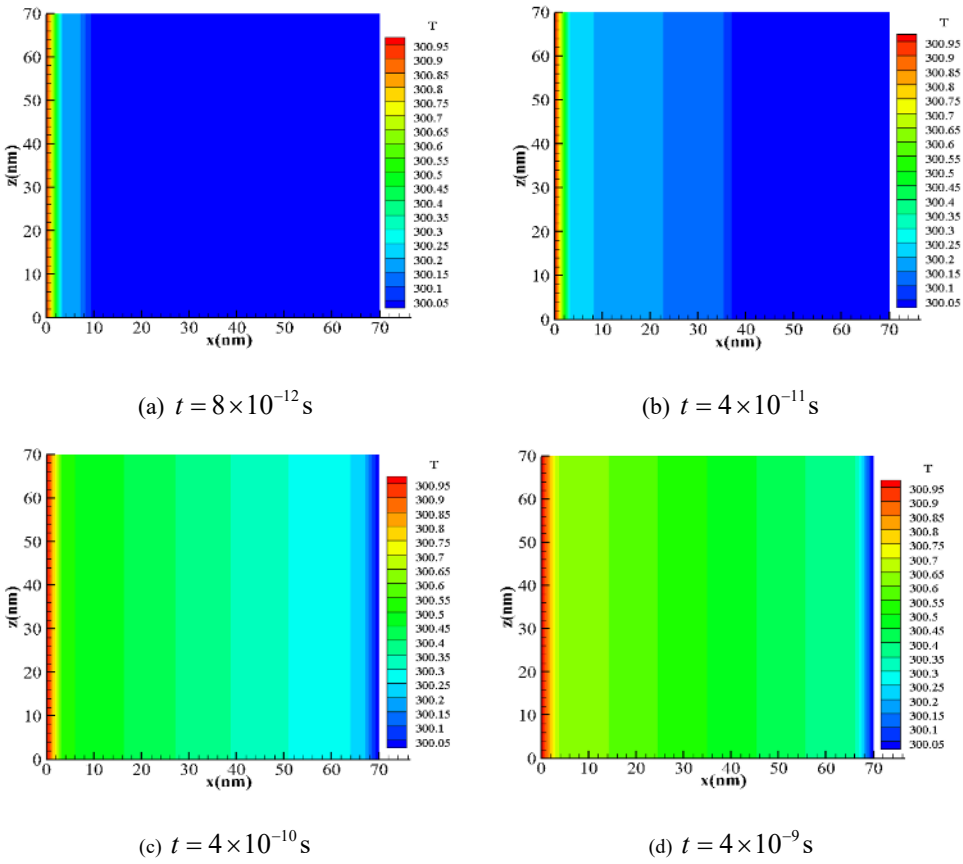

(a) $t = 8 \times 10^{-12}$s (b) $t = 4 \times 10^{-11}$s

(c) $t = 4 \times 10^{-10}$s (d) $t = 4 \times 10^{-9}$s

Fig. 3. Different t mirror boundary temperature jumps**.**

Fig.3 displayed the dimensionless steady-state temperature distribution under the value of t with the size free path of the gas molecules along the middle line in the model, the boundary was under mirror rebound boundary. It can be seen from the Fig.4 that the boundary temperature jump was mainly concentrated on high temperature area of the left side, the right side still stay constant because there is no jump when time was less than $8*10^{-12}$. When the value of t was in $8*10^{-12} \sim 4*10^{-9}$, it was obvious for the center area of the system to jump from the high temperature area to the lower, but it was not well-distributed that the left area of high temperature was relatively regular. When the value of t was the time $t=4*10^{-9}$, it is relatively regular near high temperature area because the the ratio of the mean free path was equal to which the gas molecules to the characteristic scale.

3.2 Gas diffuse reflection boundary temperature jump

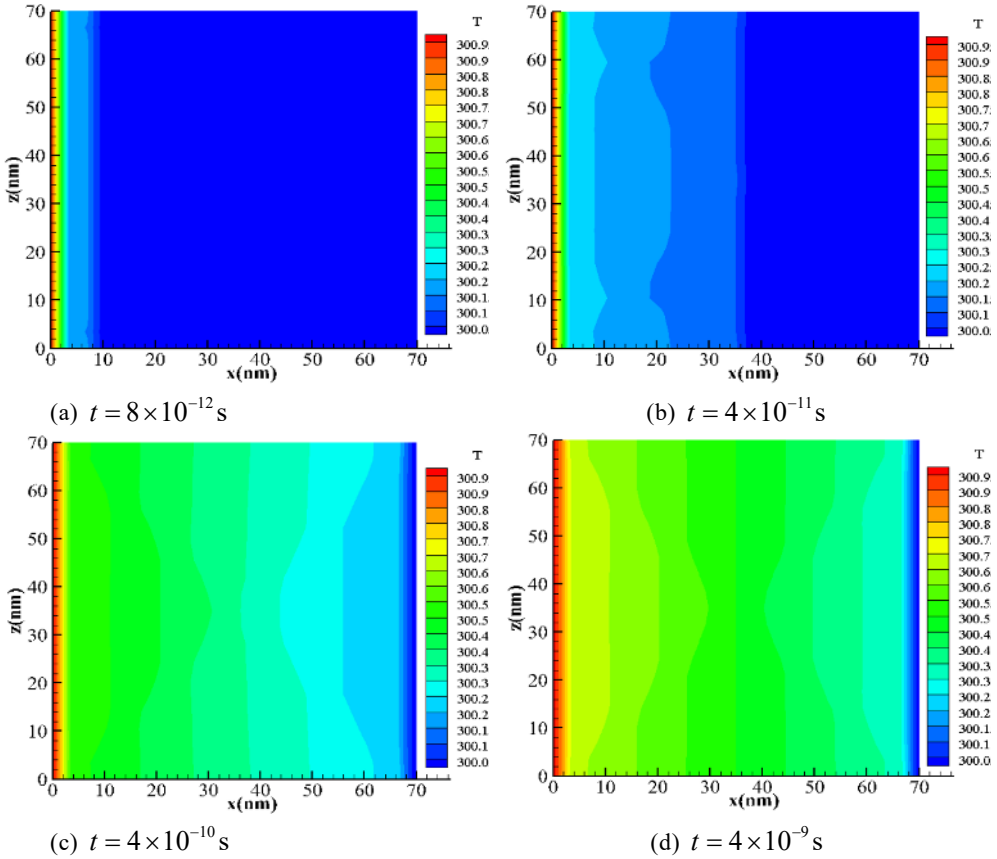

(a) $t = 8\times10^{-12}$s (b) $t = 4\times10^{-11}$s

(c) $t = 4\times10^{-10}$s (d) $t = 4\times10^{-9}$s

Fig. 4. Different t diffuse reflection boundary temperature jumps.

Fig.4 displayed the dimensionless steady-state temperature distribution under the value of t with the size free path of the gas molecules along the middle line in the model, the boundary was under diffuse reflection boundary. When the value of t was $8*10^{-12}$, the temperature jump was obvious and mainly concentrating on the high temperature area, but there was no clearly arc distribution around the boundary. With the value of t increasing slowly, it started to scatter from high temperature area to the lower area. When the value of t was $4*10^{-9}$, the system was arriving to stay stable state and the temperature jump was equal in size of both boundary.

3.3 Gas thermal conductivity

The Fig.5 showed that the effective thermal conductivity change by the value of r_b from 0~1, the value tend to decrease with the value of r_b was growing up. When r_b=0, there was neither scattering nor momentum exchange between the gas molecules and the wall, heat transfer can be achieved geratly between gases, and the thermal conductivity of gas phase is also the largest than other situations. the gas thermal conductivity can reflect heat transfer effects, the gas thermal conductivity was becoming largest owing to remove the boundary. Therefore, with the decreasing of the value of r_b, the slip velocity at the boundary was

increasing rapidly because the collision migration process between gas molexules and boundary became more and more frequently.

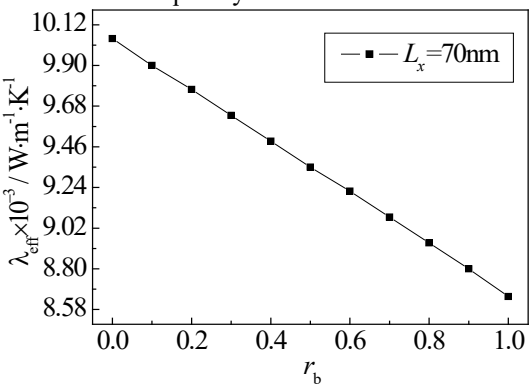

Fig. 5. Effective thermal conductivity of $\mathbf{r_b}$.

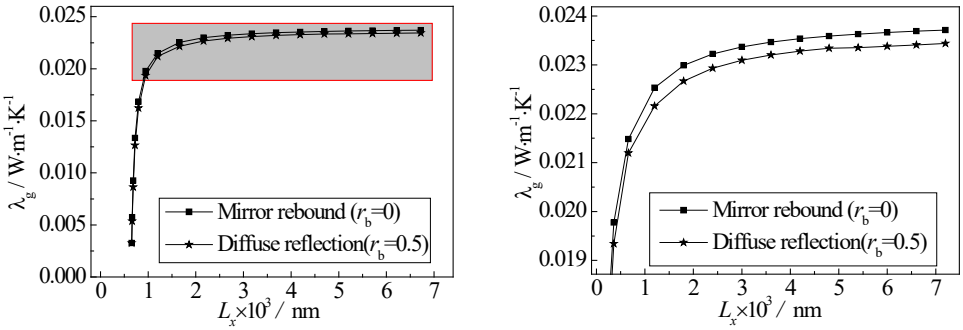

(a)Original dimension (b) Detail view

Fig. 6. Effective thermal conductivity of gas phase.

The Fig.6 showed that the effective thermal conductivity change by the size from 0~7000nm. The values trend to constant when the pore sizes were from 1000nm to 7000nm. But the effective thermal conductivities dramatically decreased when the pore sizes were less than 1000nm. The reasons were also similar to the temperature changing. We know that the gas heat conduction was carried out by the thermal movement of gas molecules, when the pore size was much larger than the mean free path of gas molecules, the gas molecules were not affected by boundary scattering and could move freely, therefore, the system will exhibit macroscopic characteristic of heat conduction. when the pore size gradually decreases, the free movement of gas molecules would be restricted by the boundary, and thermal transport would also gradually weaken between gas molecules, so the thermal conductivity displays an obvious downward trend.

4 Conclusions

In this paper, a model of the gas heat conduction aerogel was established, and the tempreture transport were studied deeply by lattice Boltzmann method. The results were as follow:

(1) When the effective thermal conductivity change by the size L_X from 1000~7000nm, the effective thermal conductivities maintained constant, the gas heat conduction was characterized by macroscopic transport and presents a uniform temperature distribution.

(2) When the effective thermal conductivity change by the size L_X less than 1000nm, the effective thermal conductivities would increase rapidly with the growth of pore size L_X. the significant temperature jumps occurred on the boundaries.

References

1. Zhang Z. H, et al. Silia aerogel materials: preparation, properties, and applications in low-temperature thermal insulation, Journal of Aeronautical Materials, 35(2015), 1, pp. 87-96.
2. Wu X. D, et al. Advance in research of high temperature resistant aerogel used as insulation material, Materials Review, 29(2015), 9, pp. 102-108.
3. Hya B, Hz A, Pb B, et al. Prediction of Thermal Conductivity of Micro/Nano Porous Dielectric Materials: Theoretical Model and Impact Factors[J]. Energy, 2021.
4. Kaganer M. G, Moscona. A. Thermal insulation in cryogenic engineering[M]. Israel Program for Scientific Translations Jerusalem, 1969.
5. Reichenauer G, et al, Relationship between pore scale and the gas pressure dependence of the gaseous thermal conductivity[J]. Colloids and Surfaces A: Physicochem. Eng. Aspects, 300(2007), 1, pp. 204-210.
6. Zeng S. O, et al. Geometric structure and thermal conductivity of porous medium silica aerogel, Journal of Heat Transfer, 117(1995), 4, pp. 1055-1058.
7. Momin A A, Shende N, Anamtatmakula A, et al. Mathematical Modeling of Heat Conduction[J]. 2021.
8. Luo Z Y, Su G H, Yang Z C. Heat conduction mechanism in silica aerogel skeleton[J]. Journal of Physics: Conference Series, 2020, 1605(1):012150 (7pp)..
9. Han Y. F, et al. Simulation on phonon heat transport of silicon dioxide nanomaterial by lattice boltzman method, Journal of Engineering Thermophysics, 32(2011), 9, pp. 1571-1574.
10. Zhu C. Y, Li Z. Y, Pang H. Q, et al. Numerical Modeling of the Gas-contributed Thermal Conductivity of Aerogels[J]. International Journal of Heat and Mass Transfer, 2018, 131(3): 217-225.
11. Li Z, Huang X, Wu K, et al. Fabrication of regular macro-mesoporous reduced graphene aerogel beads with ultra-high mechanical property for efficient bilirubin adsorption[J]. Materials science & engineering, 2020, 106(Jan): 110282.1-110282.11.
12. He Y. L, et al. Lattice Boltzmann method and its applications in engineering thermophysics, Chinese Science Bulletin, 54(2009), 18 , pp. 2638-2656.